Supporting Information

Nano-sized Porous Artificial Enzyme as pH-Sensitive Doxorubicin Delivery System for Joint Enzymatic and Chemotherapy towards Tumor Treatment

Zhilu Xu,† Ting Wang,† Jing Li,† Fang Zhang,† Han Lou, Jian Zhang, Wenhua Zhang, Weifen Zhang* Baolong Zhou**

Weifang Medical University, Weifang, 261053, Shandong, P. R. China

† These authors contribute equal to this article.

E-mail: zhoubaolong@wfmu.edu.cn

Contents

Section 1. Materials and methods

Synthesis of the HF-POP

Initially, freshly distilled pyrrole (0.48 mL, 6.96 mmol) and hexa-(4-aldehyde-phenoxy)-cyclotriphosphazene (1.0 g, 1.16 mmol) were mixed, following by the injection of propanoic acid (55 mL) and nitrobenzeneand (36 mL). Then, $FeCl_2 \cdot 4H_2O$ (0.28 g, 1.39 mmol) was added into the above mixture. Under the protection of N_2, the mixture was heated to reflux for 2 days and slowly cooled to room temperature. A black powder was obtained in the meantime. The obtained product was filtered and washed with DMF until the filtrate was colourless. Then, the as-prepared solid was frequently washed with ethanol and tetrahydrofuran. Finally, the obtained product was dried in a vacuum oven. Subsequently, the obtained solid was rigorously washed by Soxhlet extraction for 24 h with dichloromethane and methanol, respectively. Finally, the as-synthesized HF-POP was dried overnight at 120 ^{o}C in a vacuum oven.[1] (Yield: 1.36 g, 95%).

Synthesis of the HF-900

HF-900 were prepared via direct pyrolysis of Fe-chelating porous organic polymers at 900 ^{o}C at kept for 2 hours under the atmosphere of argon.[2]

Synthesis of the HF-900-DOX

DOX and HF-900 were suspended in 2 mL water with stirring at room temperature for 8 h. The mass of DOX in different mass ratio to HF-900 was 2:1, 1:2, 1:4, and 1:6, respectively. The DOX was firmly absorbed into the pores of the HF-900 during agitation, due to the structural similarity between the DOX and carries.[3]

Section 2. XPS

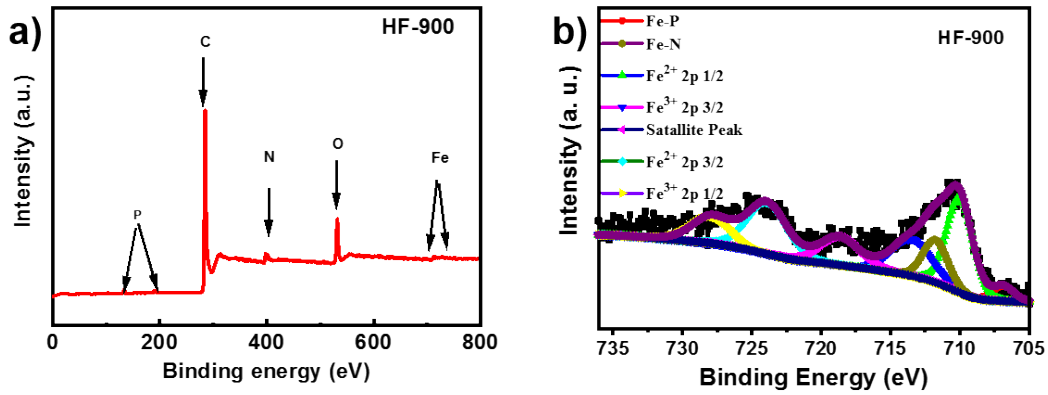

Figure S1. XPS of HF-900. a) XPS survey spectrum of HF-900; b) high resolution Fe 2p XPS of HF-900.

Section 3. Size and Zeta Potential

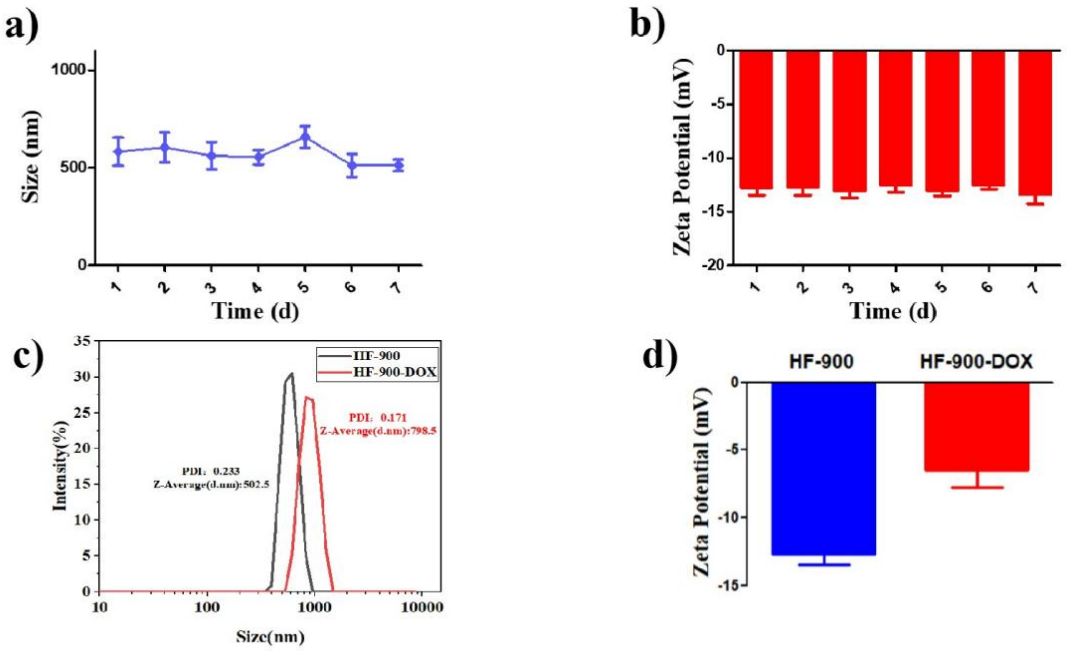

Figure S2. Size a) and Zeta Potential b) changes of HF-900 in aqueous solution at different time. Size c) and Zeta Potential d) of HF-900 and HF-900-DOX.

Section 4. The catalytic activity of HF-900 enzymes

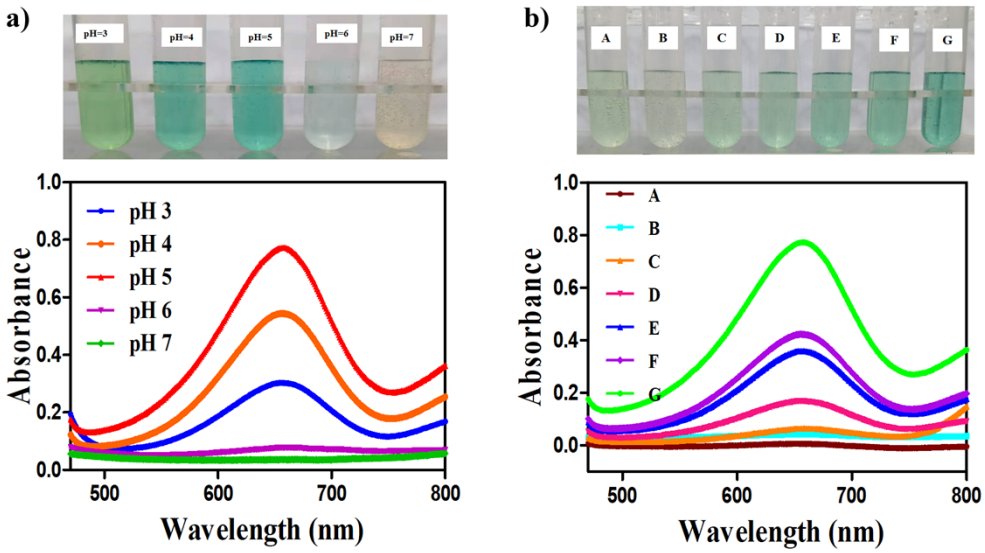

Figure S3. UV-Visible absorption spectra of different reaction systems. a) The effect of pH on absorption value with HF-900. b) The absorption value with different concentration of HF-900: (A)TMB + H_2O_2, (B) TMB + HF-900, (C) TMB + H_2O_2 + 20 μg mL^{-1} HF-900, (D) TMB + H_2O_2 + 50 μg mL^{-1} HF-900, (E) TMB + H_2O_2 + 100 μg mL^{-1} HF-900, (F) TMB + H_2O_2 + 150 μg mL^{-1} HF-900 (G) TMB + H_2O_2 + 200 μg mL^{-1} HF-900.

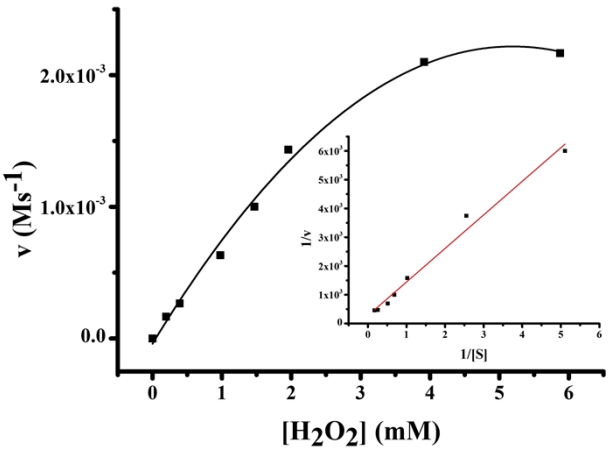

Figure S4. The enzymatic kinetic assay of HF-900 nanoparticles.

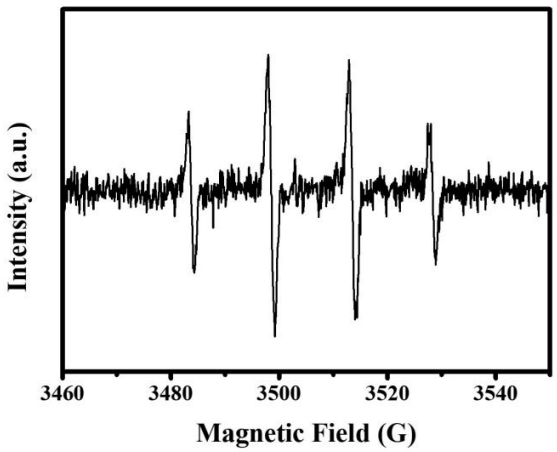

Figure S5. ESR spectra for detection of hydroxyl radical in the presence of DMPO.

Section 5. Flow cytometry assay

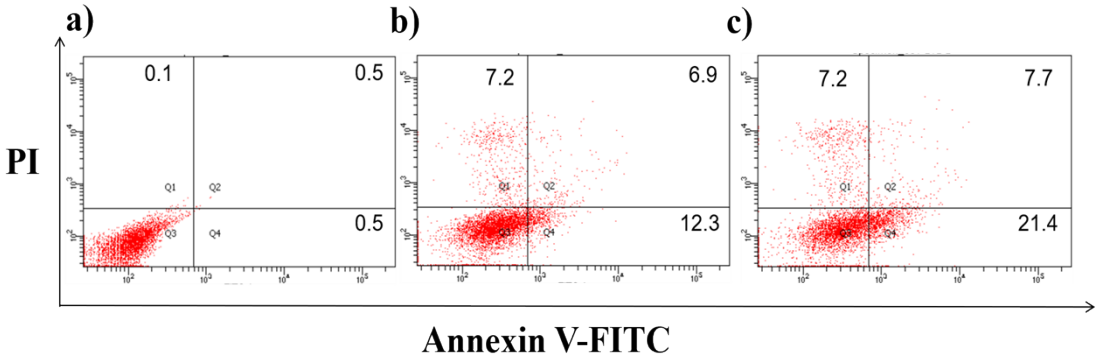

Figure S6. Analysis of 231 cells using Annexin V-FITC and Propidium Iodide,[4] 231 cells were treated with PBS (a), 100 μg mL^{-1} (b) or 200 μg mL^{-1} (c) of HF-900.

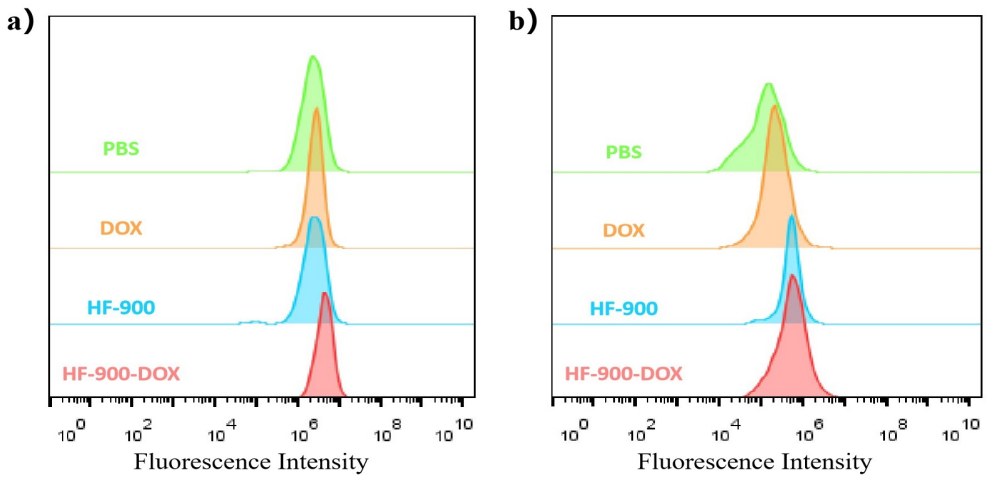

Figure S7. Flow cytometry of intracellular ROS: a) ROS expression level of 231 cells; b) ROS expression level of 4T1 cells.

Section 6. Supporting Tables

Table S1. Results of Drug Loading (%) and Encapsulation Efficiency (%) (Mean ± SD, n = 3).

mass ratio (material:drug)	loading capacity	encapsulation efficiency
2:1	15.20±2.14	35.95±5.97
1:1	19.43±2.99	24.23±4.53
1:2	23.79±2.16	15.64±1.85
1:4	49.64±2.18	24.10±2.10
1:6	61.28±3.15	26.56±3.42

Table S2. Elemental analysis[5] and ICP analysis[6] of HF-900 and HF-900-DOX. The af represents atomic fraction and the mf represents mass fraction.

Sample	C (mf%)	N (mf%)	O (mf%)	P (mf%)	Fe (mf%)
HF-900	87.8	0.7955	8.275	2.74	0.394
HF-900-DOX	91.0	0.206	7.785	0.5675	0.4635

Sample	C (af%)	N (af%)	O (af%)	P (af%)	Fe (af%)
HF-900	91.6	0.7085	6.485	1.1075	0.08815
HF-900-DOX	93.5	0.1825	6.005	0.2265	0.1027

Section 7. Supporting References

(1) Pan, Q.; Xu, Z.; Deng, S.; Zhang, F.; Li, H.; Cheng, Y.; Wei, L.; Wang, J.; Zhou, B. A Mechanochemically Synthesized Porous Organic Polymer Derived CQD/Chitosan–Graphene Composite Film Electrode for Electrochemiluminescence Determination of Dopamine. *RSC Adv.* **2019**, *9* (67), 39332–39337. https://doi.org/10.1039/C9RA06912G.

(2) Zhou, B.; Yan, F.; Li, X.; Zhou, J.; Zhang, W. An Interpenetrating Porous Organic Polymer as a Precursor for FeP/Fe 2 P-Embedded Porous Carbon toward a PH-Universal ORR Catalyst. *ChemSusChem* **2019**, *12* (4), 915–923. https://doi.org/10.1002/cssc.201802369.

(3) Liu, Z.; Li, T.; Han, F.; Wang, Y.; Gan, Y.; Shi, J.; Wang, T.; Akhtar, M. L.; Li, Y. A Cascade-Reaction Enabled Synergistic Cancer Starvation/ROS-Mediated/Chemo-Therapy with an Enzyme Modified Fe-Based MOF. *Biomater. Sci.* **2019**, *7* (9), 3683–3692. https://doi.org/10.1039/c9bm00641a.

(4) Trachootham, D.; Zhou, Y.; Zhang, H.; Demizu, Y.; Chen, Z.; Pelicano, H.; Chiao, P. J.; Achanta, G.; Arlinghaus, R. B.; Liu, J.; et al. Selective Killing of Oncogenically Transformed Cells through a ROS-Mediated Mechanism by β-Phenylethyl Isothiocyanate. *Cancer Cell* **2006**, *10* (3), 241–252. https://doi.org/10.1016/j.ccr.2006.08.009.

(5) Huo, M.; Wang, L.; Chen, Y.; Shi, J. Tumor-Selective Catalytic Nanomedicine by Nanocatalyst Delivery. *Nat. Commun.* **2017**, *8* (1), 357. https://doi.org/10.1038/s41467-017-00424-8.

(6) Liu, T.; Liu, W.; Zhang, M.; Yu, W.; Gao, F.; Li, C.; Wang, S.-B.; Feng, J.; Zhang, X.-Z. Ferrous-Supply-Regeneration Nanoengineering for Cancer-Cell-Specific Ferroptosis in Combination with Imaging-Guided Photodynamic Therapy. *ACS Nano* **2018**, *12* (12), 12181–12192. https://doi.org/10.1021/acsnano.8b05860.